Subwavelength optical spatial solitons and three-dimensional localization in disordered ferroelectrics: Toward metamaterials of nonlinear origin

C. Conti,[1,2] A. J. Agranat,[3] and E. DelRe[4]

[1]*Department of Molecular Medicine, University Sapienza, Viale Regina Elena, 324, I-00161 Rome, Italy*
[2]*Institute for Complex Systems - CNR, Department of Physics, University Sapienza, Piazzale Aldo Moro 2, I-00185 Rome, Italy*
[3]*Applied Physics Department, Hebrew University of Jerusalem, IL-91904, Israel*
[4]*Dipartimento di Ingegneria Elettrica e dell'Informazione, Universita' dell'Aquila, I-67100 L'Aquila, Italy*

(Received 27 February 2011; published 5 October 2011)

We predict the existence of a class of multidimensional light localizations in out-of-equilibrium ferroelectric crystals. In two dimensions, the nondiffracting beams form at an arbitrary low-power level and propagate even when their width is well below the optical wavelength. In three dimensions, a subwavelength light bullet is found. The effects emerge when compositionally disordered crystals are brought to their metastable glassy state, and leading to the suppression of evanescent waves, they can have a profound impact on super-resolved imaging and ultradense optical storage, resembling metamaterials in many ways.

DOI: 10.1103/PhysRevA.84.043809 PACS number(s): 42.65.Tg, 05.45.Yv, 42.65.Hw, 42.65.Jx

I. INTRODUCTION

Out-of-equilibrium materials display remarkable features, most of them still to be understood. Recent experiments in supercooled photorefractive crystals have allowed the observation of "scale-free" optical solitons [1] supported by an extremely weak diffusive nonlinearity [2–4], which becomes active through the emergence of a dipolar glass with anomalously enhanced susceptibility. These nonlinear beams have a truly remarkable feature: they are independent of size and intensity. Size independence spurns a very basic and potentially groundbreaking exploration: Are these scale-free optical beams capable of propagating even when their size is noticeably smaller than the optical wavelength?

In this article we predict that glassy photorefractive ferroelectrics [5–7] support multidimensional light localization at scales below the optical wavelength. The effect requires a huge susceptibility that can be harnessed in the out-of-equilibrium, or nonergodic phase, by acting on the previous history of the sample [1]. The finding is thus part of a still-infant field of investigation that focuses on using out-of-equilibrium optical materials to achieve different and to our knowledge, previously unexplored effects [8,9]: a *nonergodic nonlinear optics* that is rooted in statistical mechanics, material science, and nonlinear wave propagation. Subwavelength propagation overcomes a basic limit to optical imaging and microscopy, i.e., that a light field can only propagate components of its spatial spectrum within the diffraction limit. High-frequency components that correspond to details comparable to and smaller than the wavelength normally form evanescent waves that simply do not propagate. In stark contrast, in our predictions light leads to self-trapped beams of arbitrary intensity and widths for which no diffraction limit holds. These predictions are based on an intensity-independent nonlinearity which can be interpreted as the consequence of a widely tunable refractive index accompanied by a transmission of evanescent fields. Put differently, a nonlinearity-based metamaterial [10–14]. Indeed, as we show below, the overall effect can be interpreted as a nonlinearly enhanced refractive n_{eff} index, at any intensity level, such that $n_{\mathrm{eff}} = n_0 L/\lambda$, where n_0 is the bulk index, λ is the wavelength, and L is a characteristic length of medium that becomes greater than the wavelength in an out-of-equilibrium regime.

II. INTENSITY-INDEPENDENT NONLINEARITY

Our model system is a compositionally disordered and impurity-doped photorefractive relaxor ferroelectric (e.g., KLTN (potassium-lithium tantalate niobate) [5]). When it is rapidly cooled below the characteristic Burns temperature T_B, it exhibits polar nanoregions (PNR). These are highly polarizable randomly distributed ferroelectric-like regions that form a dipolar glass and provide an enormous enhancement of the photorefractive nonlinear optical response but retain very limited scattering losses [1]. The clue to the whole matter, originally discussed by Burns [15], is that the optically induced index of refraction change depends on the spatial average of the square of the crystal polarization $\mathbf{P}$. When the crystals display a zero polarization due to disorder (i.e., $\langle \mathbf{P} \rangle \approx 0$), averaging over disorder leads to a nonvanishing effect that depends exclusively on the mean square of the polarization (i.e., $\langle |\mathbf{P}|^2 \rangle$). Optical response is thus directly correlated to the underlying nature of the crystal fluctuations, which become anomalously large and dependent on the crystal history in the out-of-equilibrium state. Specifically, averaging over the randomly oriented PNR [6,7], the index of refraction perturbation is

$$\Delta n_{\mathrm{PNR}} = -\frac{n_0^3}{2} g \epsilon_0^2 \chi_{\mathrm{PNR}}^2 E_{DC}^2, \tag{1}$$

where n_0 is the bulk refractive index of the isotropic (disordered) crystals, g is the relevant component of the second-order electro-optic tensor, and χ_{PNR} is the low-frequency electric response due to the PNR.

The low-frequency electric field E_{DC} is the space-charge field expressed in terms of the optical intensity I as [1,2] $E_{DC} = -(k_B T/q)|\nabla I|/I$, with T the crystal temperature, k_B the Boltzmann constant, and q the elementary charge. Note that it is this dependence on I that bestows on all effects their characteristic intensity independence. Nonergodicity implies that χ_{PNR} will depend on the history of the sample, so that the same crystal at the same temperature will display radically different nonlinear optical responses [1]. Equation (1) holds because χ_{PNR} is several orders of magnitudes greater than the susceptibility of the crystals in the paraelectric phase χ_P, so that the nonlinear effect is mainly due to the PNR. Terms in the index perturbation that depend on the spontaneous polarization P_0 (i.e., in $\langle P_0^2 \rangle$) do not depend on the optical field, are negligible compared to the effects of the PNR, and are henceforth dropped. Finally, off-diagonal index modulation terms, that would amount to polarization rotation effects, are averaged out by the PNR disorder and hence are negligible.

III. SCALE-FREE SELF-TRAPPED PARAXIAL BEAMS

In the paraxial approximation, for a linearly polarized beam the slowly-varying optical field A ($|A|^2 = I$ is the optical intensity) obeys the nonlinear equation

$$2ik\frac{\partial A}{\partial z} + \nabla_\perp^2 A - \frac{L^2}{4\lambda^2}\frac{(\partial_x I)^2 + (\partial_y I)^2}{I^2}A = 0, \tag{2}$$

where we have introduced the characteristic length

$$L = 4\pi n_0^2 \epsilon_0 \sqrt{g}\,\chi_{\text{PNR}}(k_B T/q), \tag{3}$$

with $g > 0$ (for commonly adopted ferroelectrics) and $k = \omega n_0/c$. The resulting model admits analytical self-trapped solutions originally found in [2] and experimentally investigated in [1] if condition $L \geqslant \lambda$ is fulfilled.

We stress that the ratio L/λ measures the relative strength of nonlinearity and diffraction, as long as L is small, or vanishes, it corresponds to a negligible nonlinearity and diffraction prevails. For $L \geqslant \lambda$ self-trapped beams exist at any waist, even beyond the paraxial approximation (depending on the beam waist), as detailed below. This is inherently a nonlinear effect and disappears for $L = 0$ when the beam is subject to linear diffraction. In some respects, L plays for the nonlinearity the same role of λ for diffraction: if L grows the effect of nonlinearity is stronger. Note, however, that L is not directly related to the size of the beam w_0, which is a free independent parameter as long as the self-trapped solutions exist (i.e., for $L/\lambda > 1$).

For $L = \lambda$ one has the exact Gaussian solution $A = a\exp(-i\beta z)$, with

$$a = A_0 \exp\left(-\frac{x^2+y^2}{w_0^2}\right), \tag{4}$$

where $\beta = 2/kw_0^2$ is the nonlinear correction to the wave vector k. Remarkably, in Eq. (4) the waist w_0 of the soliton and its amplitude A_0 are free independent parameters. When $L > \lambda$ a notable effect is that self-trapped solutions are given by $A = ae^{-i\gamma^2\beta z}$, with

$$a = A_0\left[\cosh\left(\sqrt{2}\frac{x}{w_0}\right)\cosh\left(\sqrt{2}\frac{y}{w_0}\right)\right]^{-\gamma^2}, \tag{5}$$

and A_0 and w_0 arbitrary constants (i.e., the "existence curve" is flat [3]), while

$$\frac{1}{\gamma} = \sqrt{\left(\frac{L}{\lambda}\right)^2 - 1}. \tag{6}$$

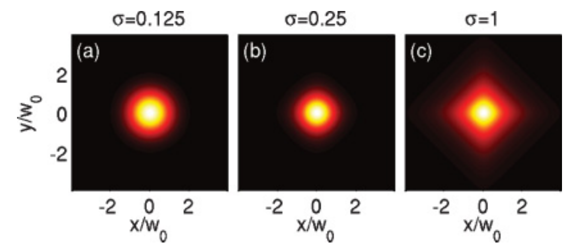

FIG. 1. (Color online) Scale-free solutions for various values of $\sigma = (L^2/8\lambda^2)$. We show the profile in (a) of the Gaussian solution ($\sigma = 0.125$) and in (b, c) of the generalized solution Eq. (5).

Interestingly, as L grows the beam loses its radial symmetry, developing a squarelike profile. In Fig. 1 we compare the two solutions.

IV. SUPPRESSION OF EVANESCENT WAVES

We consider scale-free solutions for beam waists comparable to and smaller than the wavelength. We use the Helmholtz equation, which generalizes the paraxial equation (2). The only approximation we implement is neglecting coherent vectorial coupling: this is expected to play a negligible role for isotropic disordered crystals and for the diffusive nonlinearity, which only depends on the local intensity profile and not on the beam polarization [2,3], as also can be verified by order-of-magnitude arguments on the term $\nabla\nabla\cdot\mathbf{E}$ in the vectorial wave equation. In the paradigmatic case of $L = \lambda$, we have that $\chi_{\text{PNR}} \simeq 10^5$ (see Ref. [1]) so that $\Delta n = -(gn_0^3/2)\epsilon_0^2(k_B T/q)^2/w_0^2$, is $\Delta n \simeq -3.1\times10^{-16}[m^2]/w_0^2$. As said above, the Δn is dependent on w_0, something that does *not* occur for local nonlinearities such as the optical Kerr effect. Now, in order to drop the vector-coupling term in the Maxwell solution leading to the Helmholtz equation, we must have that $w_0^2/\lambda^2 \gg \Delta n/n_0 = 3.1\times10^{-16}[m^2]/w_0^2$. In our most extreme case of $\lambda = 10^{-6}$m ($\epsilon = 0.05$, see below), $w_0 = 0.22\lambda$, so that $0.05 \gg 3.1\times10^{-16}/(0.22\times10^{-6})^2$, i.e., $0.05 \gg 0.0064$. This allows us to neglect vectorial effects even in the extreme case of $\epsilon = 0.05$ (see below). Moreover, the nature of the nonlinearity is polarization insensitive, so that even those small parts of the propagating beam that suffer polarization conversion will not, in general, produce a qualitative change in predicted phenomena.

The Helmholtz model reads as ($n = n_0 + \Delta n$)

$$\nabla^2 E + \left(\frac{\omega n}{c}\right)^2 E = 0, \tag{7}$$

whose propagation-invariant solution is written as $E = a\exp(ik_z z)$, where k_z is the overall wave vector in the z direction (different from its nonlinear perturbation β in the paraxial model above). Equation (4) is also a solution of Eq. (7), with arbitrary amplitude A_0 and waist w_0, with

$$k_z = \sqrt{\left(\frac{2\pi n_0}{\lambda}\right)^2 - \frac{4}{w_0^2}} \tag{8}$$

when the condition $L = \lambda$ is satisfied. Note that this solution exists (i.e., k_z is real) as long as

$$w_0 > \frac{\lambda}{\pi n_0}, \tag{9}$$

that is, for a beam waist that is (within multiplicative constants) greater than the wavelength λ/n_0.

The key point is that Eq. (5) is still the solution for $L > \lambda$, as occurs in the paraxial case, with wave vector

$$k_z = \sqrt{\left(\frac{2\pi n_0}{\lambda}\right)^2 - \frac{4\gamma^2}{w_0^2}}. \tag{10}$$

The corresponding lower limit for the waist is hence

$$w_0 > \gamma \frac{\lambda}{\pi n_0}. \tag{11}$$

The factor γ plays a role similar to a Lorentz contraction term in special relativity. For $L > \sqrt{2}\lambda$ the lower limit for the waist is scaled by a factor $\gamma < 1$. Note that a part of the evanescent waves (present in a beam of the same waist when $L = 0$) is now absent, so that arbitrarily low power beams with size below the wavelength can propagate. This can be described by an enhanced refractive index n_{eff}, as discussed below.

V. NONPARAXIAL REGIME

To investigate the formation of the nonparaxial two-dimensional (2D) beams, we consider the forward projection of the Helmholtz equation:

$$i\partial_z E + k\sqrt{1 + \frac{\nabla_\perp^2}{k_0^2} + 2\frac{\Delta n}{n_0}}\,E = 0. \tag{12}$$

Equation (12) reduces, under suitable limits, to the well-known unidirectional propagation equations (see [16,17] and references therein) for the description of nonlinear optics beyond the paraxial model. The basic difference here is that the nonlinear refractive index Δn is retained under the square root, since our nonlinearity is intensity-independent and hence of the same order of the Laplacian, even in the low-intensity regions of the beam. After introducing the optical carrier with $E = A\exp(ikz)$ and the diffusive nonlinearity, the normalized dimensionless model reads as the nonparaxial normalized model,

$$\begin{gathered} i\partial_\zeta \psi + \frac{1}{\epsilon}\left[-1 + \sqrt{1 + \epsilon\nabla_{\xi,\eta}^2 - 2\epsilon\sigma(\mathbf{v}\cdot\mathbf{v})}\right]\psi = 0, \\ \mathbf{v}|\psi|^2 + \nabla_{\xi\eta}|\psi|^2 = 0, \end{gathered} \tag{13}$$

where we introduce the dimensionless variables $\xi = x/w_0$, $\eta = y/w_0$, and $\zeta = z/z_0$ with $z_0 = kw_0^2$ the Rayleigh length. $\psi = A/A_0$ is the normalized optical field with A_0 an arbitrary constant, and $\mathbf{v} = \mathbf{E}_{DC}/(k_B T/q)$ is the normalized space-charge field. In Eq. (2) only two parameters appear: the degree of nonparaxiality $\epsilon = 1/(kw_0)^2$, which vanishes in the paraxial limit, and the strength of the scale-free nonlinearity σ ($\sigma = 1/8$ as $L = \lambda$).

Equation (2) can be numerically solved by Taylor expanding the square root, giving

$$\partial_\zeta \psi = i\sum_{n=1}^{N} \binom{\frac{1}{2}}{n} \epsilon^{n-1}\left[\nabla_{\xi,\eta}^2 - 2\sigma(\mathbf{v}\cdot\mathbf{v})\right]^n \psi, \tag{14}$$

where N is the order of approximation selected (for a fixed ϵ) in order to a have a given precision.

To assess the existence of self-trapped scale-free solitons beyond the paraxial regime, we start by considering the linear diffraction regime ($\sigma = 0$; $L \ll \lambda$) in Fig. 2(a), which shows the spreading of the waist of a Gaussian beam for an increasing order in the the solution of Eq. (14). For $\epsilon > 0$ nonparaxial terms provide a more pronounced spreading if compared to the paraxial model (i.e., to $N = 1$), and it is shown that for the case of $\epsilon = 0.05$ corrections become inconsequential for $N > 3$.

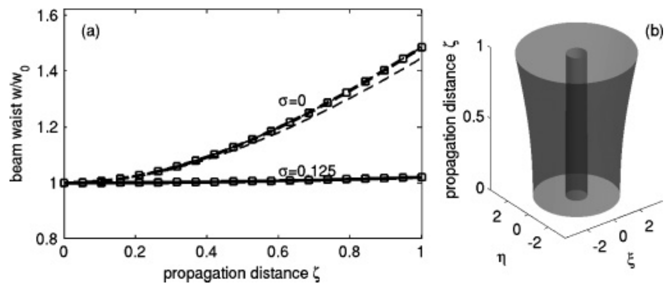

FIG. 2. (a) Beam waist versus propagation for $\epsilon = 0.05$ for various orders of approximation of the nonparaxial equations (black line corresponds to standard paraxial models). As $\sigma = 0$ the nonparaxial terms lead to a more pronounced spreading; for $\sigma = 0.125$ an invariant propagation is attained at any nonparaxial order. (b) 2D + 1 comparison between the case $\sigma = 0$ and $\sigma = 0.125$ for $N = 3$.

In Fig. 2(b) we show the propagation of the beam for $\sigma = 1/8$ ($L = \lambda$), including higher order diffraction. In such a nonlinear case, diffractionless propagation is achieved at any order and for any intensity. Note that the resulting beam is propagation invariant at any order N independently on the scale w_0 and on the intensity level, thus showing the fact that the proposed scale-free solutions are indeed stable and exist for ultrathin beams.

VI. ENHANCED VISIBILITY

We consider the propagation of two parallel beams for $\epsilon = 0.01$ (order $N = 3$) for various values of the ratio L/λ. For a given input pattern we find that there exists an optimal value corresponding to minimal input intensity distribution (i.e., image) distortion. In Fig. 3 we consider two parallel beams for different σ. We compare the [Fig. 3(b)] linear propagation regime ($\sigma = L/\lambda = 0$) and the case $\sigma = 0.15$ [Fig. 3(c)]; for $\sigma > 0$ (high cooling rates see [1]) the visibility increases.

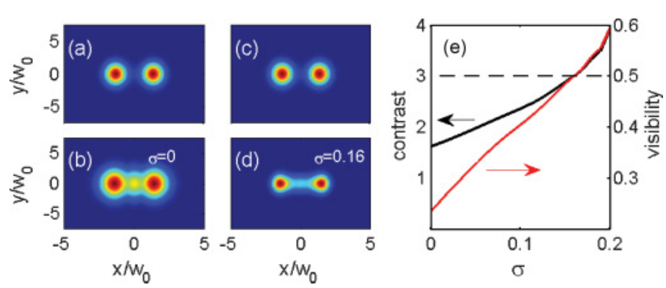

FIG. 3. (Color online) Intensity-independent super-resolution: (a,b) Propagation in the linear regime ($L = \sigma = 0$) of a double spot (panel a) in the nonparaxial model Eq. (14) at the third order ($N = 3$) with $\epsilon = 0.01$; (c, d) as in (a, b) with $\sigma = 0.2$; (e) calculated contrast and visibility versus σ. The initial image in panels (a, c) is the same and is included for the sake of comparison. Propagation distance $z = 1$.

We stress that these dynamics are attained at any intensity level and hence represent a different regime in optical propagation.

In Fig. 3(d) we show the fringe contrast and visibility versus σ, the former being the ratio between the intensity peak $I_{\max}$ and that at the center $I_{\min}$, the latter being $(I_{\max} - I_{\min})/(I_{\max} + I_{\min})$. Following the Rayleigh criterion, fringes are resolved as the visibility is greater than 0.5. Figure 3(b) shows that even for nonparaxial beams, super-resolution is possible (visibility >0.5 as $\sigma > 0.16$) by also inhibiting the loss of information due to evanescent waves.

VII. THREE-DIMENSIONAL SUBWAVELENGTH LOCALIZATION

A notable property is the existence of three-dimensional (3D) localized light bullets. Specifically, a 3D Helmholtz equation for the diffusive nonlinearity can be cast as a "nonlinear" eigenvalue problem:

$$-\frac{\nabla^2 E}{E} + \left(\frac{L}{\lambda}\right)^2 \left(\frac{\nabla |E|^2}{2|E|^2}\right)^2 = k^2. \qquad (15)$$

Equation (15) admits an *exact* 3D Gaussian solution $A = A_0 \exp[-(x^2 + y^2 + z^2)/w_0^2]$ when $L = \lambda$, for any A_0 and when $w_0 = \sqrt{3/2\pi}\lambda/n_0$. In distinction from previous results, these solutions are not spatially scale-free and may only have a fixed waist, comparable with the wavelength. For $L > \lambda$ a solution exists (more general ones will be reported elsewhere) and is given by

$$A = A_0 \left[\cosh\left(\frac{\sqrt{2}x}{w_0}\right) \cosh\left(\frac{\sqrt{2}y}{w_0}\right) \cosh\left(\frac{\sqrt{2}z}{w_0}\right)\right]^{-\gamma^2}, \qquad (16)$$

with γ as in Eq. (6) and the waist $w_0 = \gamma\sqrt{3/2\pi}\lambda/2\pi n_0$. These 3D localized solutions have a waist smaller that the wavelength when $\gamma < 1$ ($L > \sqrt{2}\lambda$). They represent a unique form of light localization at any intensity level. We are not aware of other known light localizations than can be described by an exact solution; it is a different kind of bound state between the photoinduced charges and light which may be used to store information.

VIII. METAMATERIALS OF NONLINEAR ORIGIN

In standard optics, a Gaussian beam with waist w_0 has a spectral bandwidth of the order of $1/w_0$ and the minimum waist such that the spectrum is contained in the Ewald circle (i.e., without evanescent waves) is given by λ/n_0. In the scale-free regime here considered, due to the nonergodic phase of glassy ferroelectrics, such a minimum waist is given by $\gamma\lambda/n_0$. The medium hence exhibits (for $L \gg \lambda$) an effective refractive index

$$n_{\text{eff}} = \frac{n_0}{\gamma} = n_0\sqrt{\left(\frac{L}{\lambda}\right)^2 - 1} \cong n_0\frac{L}{\lambda} \gg n_0. \qquad (17)$$

The PNR effect is therefore equivalent to an (intensity *independent*) refractive index, which can be largely tuned and increased, such that beams propagate without evanescent waves and without relevant scattering and absorption losses. This shows that the specific nonlinearity considered here is able to provide features that are the building blocks for modern research on metamaterials from a completely different perspective.

ACKNOWLEDGMENTS

We acknowledge support from the CINECA-ISCRA parallel computing initiative. The research leading to these results has received funding from the European Research Council under the European Community's Seventh Framework Program, FP7/2007-2013/ERC grant agreement No. 201766, and from the Italian Ministry of Research (MIUR) through the "Futuro in Ricerca," (FIRB), Grant PHOCOS-RBFR08E7VA, and PRIN 2009P3K72Z. Partial funding was received through the SMARTCONFOCAL Project of the Regione Lazio. C.C. acknowledges support from the Humboldt Foundation.

[1] E. DelRe, E. Spinozzi, R. Agranat, and C. Conti, Nature Photon. **5**, 39 (2010).
[2] B. Crosignani, A. Degasperis, E. DelRe, P. Di Porto, and A. J. Agranat, Phys. Rev. Lett. **82**, 1664 (1999).
[3] E. DelRe, B. Crosignani, and P. Di Porto, Prog. Opt. **53**, 153 (2009).
[4] E. DelRe and M. Segev, *Self-Focusing and Solitons in Photorefractive Media*, Vol. 114 of *Topics in Applied Physics* (Springer, Berlin, 2009), pp. 547–572.
[5] A. Agranat, R. Hofmeister, and A. Yariv, Opt. Lett. **17**, 713 (1992).
[6] A. A. Bokov and Z.-G. Ye, J. Mater. Sci. **41**, 31 (2006).
[7] G. Samara, J. Phys. Condens. Matter **15**, R367 (2003).
[8] N. Ghofraniha, C. Conti, G. Ruocco, and F. Zamponi, Phys. Rev. Lett. **102**, 038303 (2009).
[9] C. Conti and E. DelRe, Phys. Rev. Lett. **105**, 118301 (2010).
[10] V. G. Veselago, Sov. Phys. Usp. **10**, 509 (1968).
[11] N. Engheta and Ziolkowski, *Metamaterials: Physics and Engineering Explorations* (IEEE Press/Wiley-Interscience, Hoboken, NJ, 2006).
[12] J. B. Pendry, Phys. Rev. Lett. **85**, 3966 (2000).
[13] D. A. Powell, I. V. Shadrivov, and Y. Kivshar, Appl. Phys. Lett. **95**, 084102 (2009).
[14] B. A. Munk, *Metamaterials: Critique and Alternatives* (Wiley, New York, 2008).
[15] G. Burns and F. H. Dacol, Phys. Rev. B **28**, 2527 (1983).
[16] M. Kolesik, J. V. Moloney, and M. Mlejnek, Phys. Rev. Lett. **89**, 283902 (2002).
[17] C. Conti, G. Ruocco, and S. Trillo, Phys. Rev. Lett. **95**, 183902 (2005).